ARTICLE NO. 78-769

Shock Tube as a Device for Testing Transonic Airfoils at High Reynolds Numbers

William J. Cook*
Iowa State University, Ames, Iowa
and
Leroy L. Presley† and Gary T. Chapman‡
NASA Ames Research Center, Moffett Field, Calif.

A performance analysis of gas-driven shock tubes shows that transonic airfoil flows with chord Reynolds numbers in the range of 10^8 can be generated behind the primary shock in a large shock tube. A study of flow over simple airfoils has been carried out at low and intermediate Reynolds numbers to assess the testing technique. Results obtained from Schlieren photos and airfoil pressure measurements show that steady transonic flows similar to those observed for the airfoils in wind tunnels can be generated within the available testing time in a shock tube with either properly contoured test section walls or a properly designed slotted-wall test section. The study indicates that the shock tube is a useful facility for studying two-dimensional, high Reynolds number transonic airfoil flows.

Nomenclature

a = sonic velocity
A_f = airfoil frontal area
A_s = slot area, $(n)(s)(x_b)$, Fig. 9
A_{ts} = test section cross-sectional area, $(H)(W)$, Fig. 9
A_w = wall area, $(x_b)(W)$, Fig. 9
c = airfoil chord length
C_p = pressure coefficient, Eq. (5)
d = slot spacing, Fig. 9
H = test section height
m = molecular weight
M = Mach number
M_s = primary shock wave Mach number, U_s/a_1
M_2 = test Mach number, u_2/a_2
n = number of slots per wall
P = pressure
Re_c = chord Reynolds number, $u_2\rho_2 c/\mu_2$
R_u = universal gas constant
s = slot width, Fig. 9
t = time
t' = time, $t'=0$ when primary shock is at airfoil leading edge
t_i = ideal testing time, Fig. 1
T = absolute temperature
u_2 = region 2 gas velocity relative to airfoil
U_s = speed of primary shock wave
W = test section width
x = distance in flow direction
x_m = model distance, Fig. 1
y = distance perpendicular to x
α = angle of attck
γ = specific heat ratio
ρ = density
μ = coefficient of viscosity

Subscripts

1 = test gas, region 1, Fig. 1
2 = test gas, region 2, Fig. 1
4 = driver gas, region 4, Fig. 1
ij = $(\ )_i/(\ )_j$
∞ = undisturbed flow remote from airfoil

I. Introduction

AIRFOIL chord Reynolds numbers for certain advanced transonic aircraft range to nearly 10^8 (Ref. 1). Such Reynolds numbers exceed the performance capabilities of existing wind tunnels by at least a factor of three. Steps are presently being taken to correct this deficiency by constructing a cryogenic wind tunnel.[2] There is a need, however, for a smaller, less costly high-Reynolds number transonic testing facility, particularly one in which research and testing of two-dimensional transonic airfoils can be carried out in order to provide fundamental flow data and to augment analytical studies of transonic airfoil flows. One device that shows promise in fulfilling these requirements is the shock tube. This paper considers the various aspects of the use of a shock tube as a testing facility for studying the behavior of transonic airfoil flows at high Reynolds numbers.

Shock tubes have not been employed extensively in the testing of airfoils. A few studies involving the use of shock tubes in relation to airfoil testing have been performed, however. These have been reported in Refs. 3-6. In each of

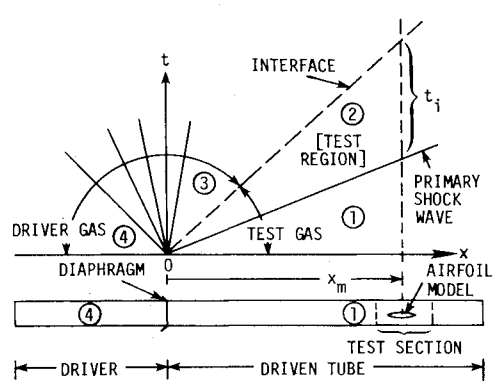

Fig. 1 Shock tube schematic diagram.

Presented as Paper 78-769 at the AIAA 10th Aerodynamic Testing Conference, San Diego, Calif., April 19-21, 1978; submitted July 20, 1978; revision received Feb. 8, 1979.

Index categories: Transonic Flow; Testing, Flight and Ground.

*Professor, Mechanical Engineering and Engineering Research Institute. Member AIAA.
†Chief, Aerodynamics Research Branch. Member AIAA.
‡Staff Scientist, Aerodynamics Division. Member AIAA.

these studies the flow behind the primary shock wave served as the test region. Results seem to indicate that airfoil testing is feasible in shock tubes. However, these investigations have been limited to low Reynolds number flows and have not adequately dealt with questions of the time required to establish steady flow, the quality of the steady flow, and the validity of data obtained in shock tubes at high subsonic speeds when compared with data obtained in conventional transonic wind tunnels. The present study was undertaken to investigate in detail the practicality of carrying out high-Reynolds number transonic airfoil testing in shock tubes. The nominal test Mach number for this study was 0.85. The simple airfoil profiles considered in this investigation exhibit supercritical flows at this Mach number.

II. Performance Analysis

It is useful to examine the performance characteristics of shock tubes in the flow regime of interest. Figure 1 presents a schematic diagram of a conventional gas-driven shock tube with an airfoil model with a chord length c mounted at a distance x_m from the diaphragm. The upper part of the figure illustrates ideal shock-tube performance in the t-x plane. Region 2, the flow region between the primary shock wave and the driver-test gas interface is the test region. The driven tube is of constant cross-sectional area except at the test section which, as will be discussed in detail, generally requires geometric modification to account for blockage effects due to the presence of the model. A rectangular cross section is preferred since it most readily produces two-dimensional flows.

Reference 7 provides the theoretical basis for predicting ideal shock-tube performance. The quantities of interest are the Mach and Reynolds numbers of the flow relative to the airfoil, the testing time, and the driver-to-driven gas pressure ratio. Generally, similarity considerations require that the Mach and Reynolds numbers and the specific heat ratio γ in the test facility be the same as those that exist in flight. Certain gases such as argon and Freon 12 (dichloro-difluoro-methane) can be mixed to yield a gas mixture with $\gamma = 1.4$, which, as a result of a larger molecular weight, offers an advantage over air for high-Reynolds number aerodynamic testing in shock tubes.

The following equations describe shock-tube performance for a general test gas. Considering the shock Mach number M_s to be the independent variable, the test Mach and Reynolds numbers and the ideal testing time per unit model distance can be written as

$$M_2 = [M_s(\rho_{21} - 1)/\rho_{21}]/(T_{21})^{1/2} \tag{1}$$

$$Re_c/cP_1 = (M_s/\mu_2)(\gamma_1 m_1/R_u T_1)^{1/2}(\rho_{21} - 1) \tag{2}$$

and

$$t_i/x_m = (m_1/\gamma_1 R_u T_1)^{1/2}/\{M_s(\rho_{21} - 1)\} \tag{3}$$

In Eq. (1), the density and temperature ratios across the shock, ρ_{21} and T_{21}, are functions of M_s and γ_1 only, since ideal gases with constanct specific heats are assumed. In Eqs. (2) and (3), m_1 is the molecular weight of the test gas, and in Eq. (2), c is a characteristic model length, i.e., the airfoil chord length. The driver-to-driven gas pressure ratio P_{41} may be written as

$$P_{41} = P_{21}/\left[1 - \frac{(P_{21} - 1)(\gamma_4 - 1)a_{14}}{(4\gamma_1^2 + 2\gamma_1(\gamma_1 + 1)(P_{21} - 1))^{1/2}}\right]^{\beta} \tag{4}$$

where P_{21} is the pressure ratio across the primary shock, $\beta = 2\gamma_4/(\gamma_4 - 1)$ and $a_{14} = (T_1\gamma_1 m_4/T_4\gamma_4 m_1)^{1/2}$.

Figure 2 presents the quantities in Eqs. (1-4), in terms of M_s, for two test gases of different molecular weight but with $\gamma_1 = 1.4$: air and a mixture of argon and Freon 12 ($\chi = 0.85$, $m_1 = 52.1$, where χ is the mole fraction of argon in the mixture that yields $\gamma = 1.4$). The driver gas is assumed to be helium. Both the driver and driven gases were assumed to be initially at room temperature.

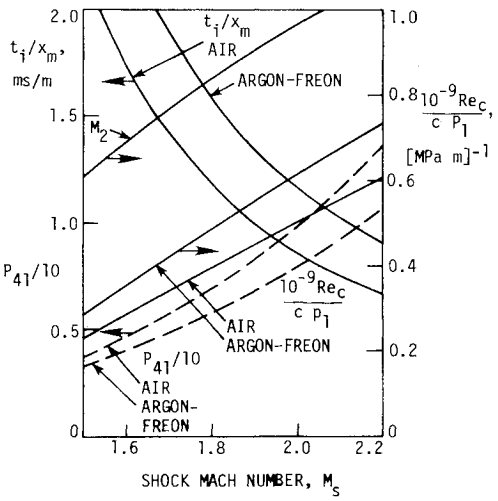

Fig. 2 Shock tube performance; driver gas: helium, test gas: air or argon-Freon 12 mixture. $\gamma_1 = 1.4$.

The curve M_2 vs M_s is the same for each test gas. From the curves and equations, it can be seen that, for a given test gas, the test Mach number M_2 can be varied by varying P_{41}. The Reynolds number for a given model can be varied independently by varying P_1.

A preliminary evaluation of shock-tube performance for high Reynolds number transonic testing can be made on the basis of the curves in Fig. 2. Considering the case $M_2 = 0.85$ ($M_s = 1.82$), a model chord length of 15 cm, and a chord Reynolds number $Re_c = 100 \times 10^6$, values required for P_1 and P_4, determined from Fig. 2 for air as the test gas, are, respectively, 1.63 and 11.5 MPa (16 and 113 atm). Corresponding values for the argon-Freon 12 mixture as the test gas are 1.35 and 8.0 MPa (13.3 and 79.3 atm). These pressures pose no insurmountable structural problems in shock-tube design. (The large shock tube described in Ref. 8 is capable of operating at these pressures.) Thus, transonic flows with very high Reynolds numbers can, at least in theory, be generated in shock tubes. At a fixed test Mach number, the dynamic pressure in a shock tube is proportional to the unit Reynolds number. Thus, testing at the noted conditions would involve relatively high dynamic pressures that would result in high model loads when lifting airfoils are tested. Calculations indicate that model support devices can be designed to carry the loads. However, model deflection may present a problem at high Reynolds numbers.

There are two additional considerations related to test-section flow that are important. One is the well-known influence of facility walls on the flow around the model. This topic requires experimental investigation and will be discussed in the next section. The other involves the time required to establish steady flow over the model. A representative testing time can be obtained using the t_i/x_m curve for air in Fig. 2. At a test Mach number of 0.85 and for a typical value for x_m of 10 m, the ideal testing time is 11 ms, about half of which would be realized in practice. Thus, shock-tube testing times would be a few milliseconds in duration. The time required to establish steady flow over a model mounted in a shock tube is difficult to determine analytically. Hence, an important aspect of the experimental phase of this investigation was to determine if steady transonic airfoil flows could be achieved within the available testing time. The next section describes the experimental phase of this study, part of which has been previously reported in Ref. 9.

III. Experimental Study

Facility Description

The shock tube used in this investigation has a driven section with a rectangular cross section 15.2 cm in height and 7.6 cm in width and a length of 9.8 m and is located in the Shock-Tube Laboratory at Iowa State University. The model station is 8.6 m from the diaphragm. The test section is 0.46 m in length and extends 0.18 m upstream of the midchord point of the airfoil. A large dump tank is attached to the downstream end of the driven tube. Mylar diaphragms ranging in thickness from 0.05 to 0.38 mm were used. A diaphragm spear was used (as opposed to allowing the diaphragms to burst naturally), in order to allow precise regulation of the pressure ratio P_{41} and accurate control of the test Mach number. Measurement of the shock speed and the initial test gas pressure and temperature permitted the test region (region 2, Fig. 1) flow properties, and hence Mach and Reynolds numbers, to be computed. A small correction was included to account for primary shock-wave attenuation. At the nominal test Mach number of 0.85 considered in this study, the facility permitted the generation of flows with Re_c values up to 2×10^6. Using air as both the driver and the test gas, the values of P_1 and P_4 required to produce this Reynolds number were, respectively, 64.7 and 1380 kPa (0.64 and 13.6 atm). Structural considerations limited the Reynolds number. A Reynolds number of 2×10^6 is adequate for investigating the testing concept, since this Reynolds number is large enough to produce a turbulent boundary layer on the airfoil upstream of the shock-wave boundary-layer interaction.

Airfoil Models

In the course of this study three symmetrical airfoil profiles were studied: the 12% thick circular-arc profile and the NACA 0012 and 64A010 profiles. The nominal chord length was 7.6 cm. This length represents a compromise between the desire to keep the airfoil small in order to minimize wall interference effects and the need for a larger size to permit accurate machining and internal mounting of instrumentation. The chosen length resulted in a nominal span-to-chord ratio (aspect ratio) of unity and placed the upper and lower test section walls approximately one chord above and below the airfoil.

Two methods were employed to study the airfoil flow. One method involved mounting the airfoils between 2-cm-thick glass windows and use of Schlieren photography. The other method consisted of the use of small fast response pressure transducers mounted on the surface of, or internal to, certain of the airfoils to measure the pressure variation with respect to both time and position on the airfoils.

Testing Time

In order to establish the actual testing time available, a constant-temperature hot-wire anemometer was used to determine the time interval between the arrival of the shock wave at the model station and the arrival of the turbulent contact region that forms between the driver and driven gases. The experimentally determined turbulence-free testing times were found to be about 40% of the corresponding ideal times. At the nominal test Mach number of 0.85, the actual test time was about 3.5 ms. The hot-wire measurements provided evidence of extremely uniform and disturbance-free flows for the duration of the measured testing time.

Wall Boundary Layers

In view of the relative sizes of the model and cross-sectional area of the test section involved, it is important to consider the thickness of the boundary layers that form on the shock tube walls in region 2, the test region. These boundary layers grow in an unsteady manner in a reference frame fixed to the model, but may be considered steady in a coordinate system attached to the moving primary shock. At the high Reynolds numbers of interest here, the wall boundary-layer flow is turbulent. Mirels[10] has treated the shock-tube sidewall turbulent boundary layer in detail. Computations based on Mirels' method show that the wall boundary-layer thickness at a fixed point in the test varies with unit Reynolds number Re_u in the form $Re_u^{-0.2}$ for a given test Mach number; i.e., the thickness decreases with increasing unit Reynolds number. In the present tests at $Re_c = 2\times10^6$, each of the two sidewall boundary layers covers 23% of the span of the airfoil. Since in turbulent boundary layers the major portion of the velocity deficit is near the wall, no large velocity gradients were indicated in the spanwise direction for the major portion of the span.

Test Section Configuration

As noted above, a well-known and important consideration in transonic testing is the influence of the test section walls on the flow around the model. This consideration is discussed extensively for conventional wind tunnels in Ref. 11. In the present study, only the influence of the test section walls above and below the model was considered. The relative size of the airfoil in relation to the test section is characterized by two ratios: the test section half-height to the airfoil chord length, $H/2c$, and the airfoil frontal area to the test section cross-sectional area, A_f/A_{ts}. The latter ratio is a measure of the blockage that occurs due to the presence of the airfoil.

For a nominal chord length of 7.6 cm and a typical 12% thick airfoil, $H/2c = 1.0$ and $A_f/A_{ts} = 0.06$. Transonic airfoil testing in most wind tunnels is carried out at smaller values of A_f/A_{ts} and larger values of $H/2c$. Accordingly, wall interference effects more pronounced than those encountered in wind tunnels would be expected in the present shock-tube test section. Two methods were employed to deal with the wall interference problem. These were: 1) the use of contoured test section walls to match streamlines close to those that occur in free flight, and 2) the use of a slotted-wall test section. The experimental investigations related to each of these methods will be discussed separately.

Contoured-Wall Tests

Shock-tube studies of the flow over two airfoil profiles were conducted using test sections with contoured walls. In each case a numerical computation technique was used to compute approximate two-dimensional stream surfaces, and the resulting surfaces were machined into blocks that form the upper and lower walls of the shock-tube test section. Although the wall contours may only approximate the real stream surfaces and therefore may not exactly reproduce airfoil flows as they would exist in free flight, this method has the distinct advantage of creating an experimental flow with known boundary conditions against which results of future transonic computational schemes can be compared.

Initial tests using contoured walls (reported in part in Ref. 9) involved testing a 12% thick circular-arc airfoil with a 7.6 cm chord at zero angle of attack. Updated results that account for primary shock wave attenuation are reported here. Two-dimensional potential-flow stream surfaces for the flow one chord length above and below the model were obtained by the methods of Murman and Cole[12] and Murman[13] for the test airfoil at Mach numbers of 0.83, 0.85, and 0.87. The influence of the displacement thickness of the turbulent sidewall boundary layer was included in determining the final wall contours. The contours extended the length of the test section (1.8 chord lengths upstream to 4.2 chord lengths downstream of the airfoil leading edge).

The flow development over the circular-arc airfoil was studied in detail by means of Schlieren photography. Figure 3a shows a photo of the primary shock wave and the wave pattern present at $t' \simeq 0.08$ ms, where $t' = 0$ when the shock arrives at the airfoil leading edge. The circular wave in Fig. 3a continues to grow and in turn reflects from the upper and lower walls as the primary shock wave moves downstream.

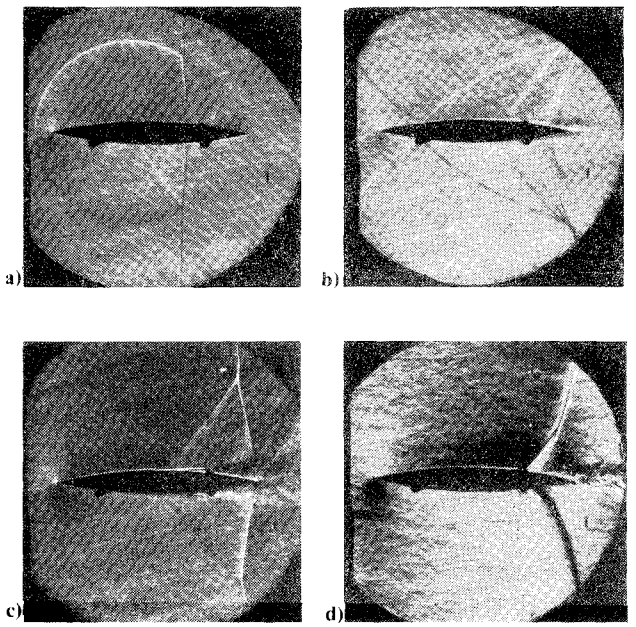

Fig. 3 Schlieren photos, circular-arc airfoil. $M=0.85$ contoured walls, $c=7.6$ cm, $M_2\simeq 0.85$, $\alpha=0$, a) $t'=0.08$ ms, b) $t'=0.50$ ms, c) $t'=2.5$ ms, $Re_c=0.27\times 10^6$, d) $t'=2.5$ ms, $Re_c=2\times 10^6$.

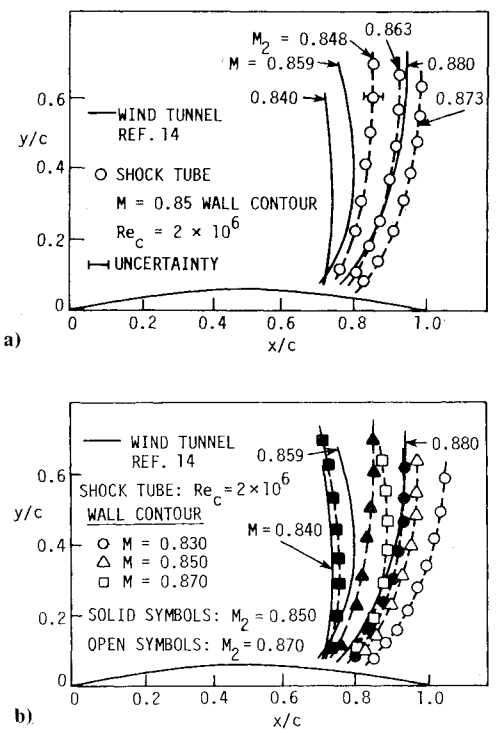

Fig. 4 Comparison of shock-wave profiles for circular-arc airfoil, $\alpha=0$.

Figure 3b shows the wave pattern at $t'=0.5$ ms. At the nominal test Mach number of 0.85, the photos showed that steady flow was established at a value of t' between 1.5 and 2.0 ms. Thus, the Schlieren photos indicated that steady flow patterns were established within the available testing time which, as previously noted, was 3.5 ms. Figures 3c and 3d show the steady flow patterns observed for two Reynolds numbers. As can be seen, there is a marked influence of Reynolds number. Figure 3c shows a low Reynolds number flow with a laminar boundary layer entering the adverse pressure gradient region on the airfoil. The flow pattern in Fig. 3c exhibits all of the features of low Reynolds number

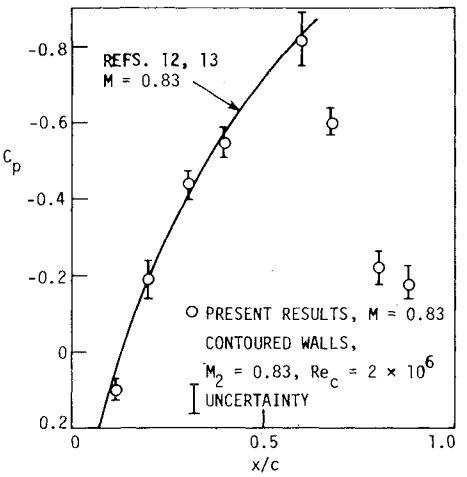

Fig. 5 Circular-arc airfoil pressure coefficients vs chord position, $\alpha=0$.

flow over the same airfoil profile observed in a wind tunnel by Wood and Gooderum.[14] Figure 3d shows a photo of a flow at $Re_c=2\times 10^6$ in which boundary-layer transition occurred upstream of the adverse pressure gradient region.§ Here the shock wave configuration is different from that in Fig. 3c, as is the wake flow. This flow pattern is similar to that observed by Wood and Gooderum in a wind tunnel for a turbulent airfoil boundary-layer flow upstream of the adverse pressure gradient region. The symmetry of the flows above and below the airfoil in the photos in Fig. 3 demonstrates that extremely uniform transonic flows are generated in the shock tube.

Shock-wave profiles like those in Fig. 3d permit comparison with shock-wave profiles observed by Wood and Gooderum[14] for turbulent airfoil boundary-layer flow. Such comparisons provide one quantitative means of evaluating the present experimental method. Figure 4a presents a comparison of steady-flow shock profiles, measured from Schlieren photos taken at various M_2 values using the $M=0.85$ wall contour, with those determined from interferograms obtained by Wood and Gooderum. An estimate of the typical uncertainty in the shock position is shown in the figure. Figure 4b shows a similar comparison that permits the influence of wall contour to be assessed. It is seen from Fig. 4 that the shock profiles for the present study exhibit fair agreement with wind tunnel results; the present profiles lie somewhat downstream of the expected positions at larger values of y/c. The results in Fig. 4b indicate that results are somewhat sensitive to the wall contour.

Further study of circular-arc airfoil flow was carried out using a separate circular-arc airfoil instrumented with pressure transducers. Small fast-response Kulite pressure transducers (Model LQL-080-25) were placed at midspan of the airfoil flush with the surface in 5 mm-wide spanwise surface grooves at various values of x/c. Paraffin wax was used to fill the voids in the grooves and maintain the airfoil profile. Transducer response records indicate that steady pressure values were reached at about 1.5 ms after shock arrival. This is in good agreement with the time required to reach steady state as determined by Schlieren photography.

Figure 5 presents a comparison of pressure coefficients C_p vs chord position determined from measured steady airfoil pressure values and those computed for the circular-arc airfoil by the methods of Refs. 12 and 13. (This comparison was made since wind tunnel pressure coefficients are not available at the Mach and Reynolds numbers at which the airfoil was

§The flowfield turbulence evident in Figs. 3d and 6 is due to the presence of turbulent sidewall boundary layers on the test section windows.

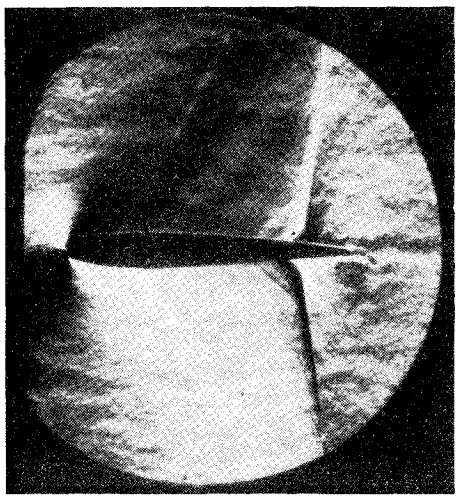

Fig. 6 Schlieren photo, NACA 0012 airfoil. $M=0.85$ contoured walls, $M_2=0.85$, $c=7.6$ cm, $Re_c=2\times10^6$, $\alpha=0$.

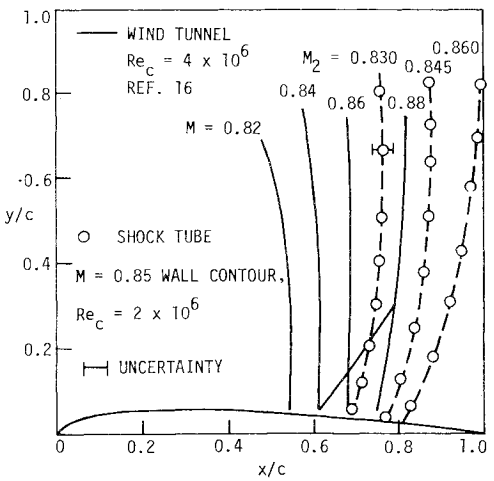

Fig. 7 Comparison of shock wave profiles for NACA 0012 airfoil, $\alpha=0$.

tested.) In the pressure coefficient expression

$$C=\frac{P-P_\infty}{\frac{1}{2}\rho_\infty u_\infty^2}=\frac{(P/P_\infty)-1}{\gamma M_\infty^2/2} \tag{5}$$

the quantities with the subscript ∞ were taken as those computed behind the primary shock, subscript 2. The uncertainties shown in the figure were determined from C_p values for various runs. The rather large uncertainty intervals were due to unavoidable roughness associated with the transducer mounting method, which tended to produce scatter in the data. Nonetheless, upstream of the shock-wave boundary-layer reaction, where the potential flow solution is expected to be applicable, the measured values agree well with the predicted curve.

A 7.6 cm chord NACA 0012 airfoil was also tested at zero angle of attack using contoured walls. This profile was chosen because wind-tunnel data were available for comparison purposes. The contour for the walls was computed using a transonic computer code[15] and was machined into the upper and lower wall blocks of the test section. As with the circular arc airfoil, both Schlieren photos and measured airfoil pressure distributions were used to study the flow. For the 0012 airfoil used in the pressure distribution study, six Kulite pressure transducers were mounted internal to the model; these sensed the surface pressure through short small-diameter holes drilled to the airfoil surface at midspan. This

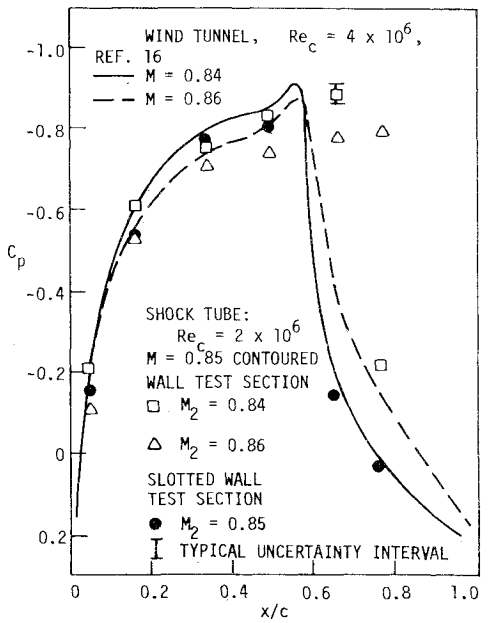

Fig. 8 Pressure coefficients vs chord position, NACA 0012 airfoil, $\alpha=0$.

proved to be a more satisfactory arrangement than the surface grooves used to install the pressure transducers on the circular arc model, in that significantly less scatter in results occurred.

Figure 6 shows a Schlieren photo of steady flow for the 0012 airfoil obtained in the contoured-wall test section at $M_2=0.85$ and $Re_c=2\times10^6$. Faint Mach lines indicating the extent of the supersonic region can be seen in the photo. Figure 7 presents a comparison of shock-wave profiles for the NACA 0012 airfoil observed in the contoured-wall test section at $Re_c=2\times10^6$ and profiles obtained from Schlieren photos taken in wind tunnel tests of this airfoil conducted by Stivers[16] in the NASA Ames Research Center 2×2 ft Transonic Wind Tunnel at $Re_c=4\times10^6$ using a 15.2 cm chord length model. Figure 8 presents a comparison of pressure coefficients vs chord position, obtained for the 0012 airfoil in the contoured-wall test section and in the wind tunnel. A typical uncertainty interval for the present C_p values is shown. The shock-tube results agree with the wind-tunnel results near the airfoil leading edge and tend to disagree as the trailing edge is approached. The results for the contoured-wall tests in both Figs. 7 and 8 indicate that the shock waves in the shock-tube tests are displaced downstream of the corresponding shock waves observed in the wind tunnel. This suggests that the blockage has not been sufficiently alleviated by the wall contours used and that less confining walls are required.

Although the results for the contoured-wall test section studies for each airfoil tested depart somewhat from the flow results expected, the method does show that steady flows near to those observed in wind tunnels can be generated in shock tubes. The present results suggest that a different wall contour should be used for each flow case; i.e., for each airfoil profile, angle of attack, Mach number, and possibly each Reynolds number. However, the contoured-wall method of testing does provide test results, for which a flow boundary condition away from the airfoil is known, that are of use in analytical and numerical studies.

Slotted-Wall Tests

In order to provide testing flexibility, a shock-tube slotted-wall test section similar to those used in wind tunnels to diminish wall effects has been developed. The objective was to provide a single test section that would accommodate various airfoil profiles and provide automatic flow compensation to minimize or eliminate wall effects. Although such test sections

have been used extensively in transonic wind tunnels,[11] they have not to the authors' knowledge been used previously in aerodynamic testing in shock tubes.

Ventilated test sections for wind tunnels typically consist of walls with open areas and relatively large adjacent chambers which, when properly designed in combination, produce test section flows around models very near to those that would exist in free flight. Generally, the slotted-wall test section is preferred for subsonic flows and flows with Mach numbers slightly above unity, and therefore was the type chosen for development for transonic airfoil testing in the shock tube. Important differences exist between transonic flows in slotted wind tunnels and those produced in shock tubes. As a result, slotted wind tunnel design features could be used only as guides in the present study.

Figure 9 shows a diagram of the general features of the slotted-wall shock-tube test section. As with the contoured-wall test section, an important feature related to the performance of the slotted-wall test section is the relative sizes of the airfoil and the test section, characterized by the ratios $H/2c$ and A_f/A_{ts}. Additional considerations for the slotted-wall test section include the wall slot geometry and the chamber size and configuration. Chambers for wind tunnel test sections are usually relatively large (of the order of the test section volume). In view of the 3.5 ms testing time in the present study, the chamber volume (characterized by x_b, y_a, and W in Fig. 9) must be of such size that steady flow is attained both in the test section and in the chamber well within the testing time. Due to the differences between transonic testing in the wind tunnel and the shock tube, the present test section, Fig. 9, was designed to permit the study of different combinations of variables affecting test section performance.

Flows over the 7.6 cm chord, 12% thick circular-arc airfoil ($A_f/A_{ts}=0.060$, $H/2c=1.0$) at zero angle of attack with a nominal Mach number of 0.85 and a chord Reynolds number of 2×10^6 were studied for different slot and chamber geometries. Results in terms of flowfields observed by Schlieren photography were compared to corresponding results obtained in the wind tunnel and in the shock tube with contoured test section walls. Initially, tests were carried out with three slots per wall, each slot 0.32 cm in width, extending the length of the test section ($d/s=7.9$, $A_s/A_w=0.13$). Early tests with chamber volume one half the test section half-volume produced unsteadiness due to reflected waves in the chambers. Reduction in chamber volume, changes in chamber configuration, and experimentation with 0.32-cm slots (ranging in number from three to five) eventually produced steady flows of 2 ms duration for the 7.6 cm-chord airfoil that agreed well with the reference flows. The experiments indicated that chamber length, height, and position are the most influential variables. The final configuration consisted of four 0.32-cm-wide slots of effective length x_b and chambers with dimensions $x_a=9$ cm, $x_b=15$ cm, $y_a=0.5$ cm and $W\simeq7.6$ cm, yielding $A_s/A_w=0.17$ and $d/s\simeq5.9$ (see Fig. 9).

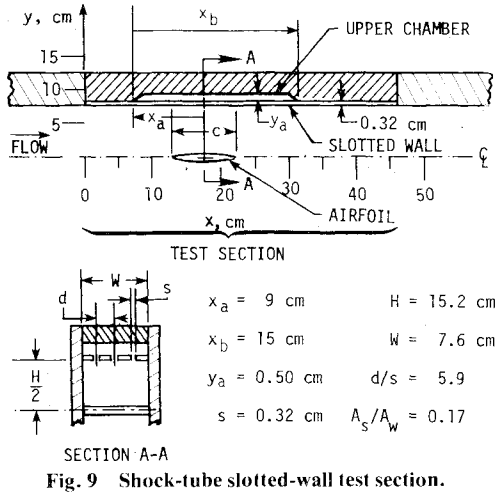

Fig. 9 Shock-tube slotted-wall test section.

Figure 10 shows shock profiles obtained for the 7.6 cm circular-arc airfoil in the previously described slotted-wall test section. Also shown are the wind-tunnel shock profiles and a shock profile observed at $M_2=0.85$ in the contoured-wall test section. The figure shows good agreement between the slotted-wall and wind tunnel shock profiles. Pressure coefficients at five positions on the circular-arc airfoil were obtained at $M_2=0.85$ using the slotted-wall test section and compared with corresponding measurements made under the same flow conditions using the same model in the contoured-wall test section. The comparison showed good agreement between the two sets of data. Thus, for the circular-arc airfoil, flows near to those observed in the wind tunnel were produced in the shock tube slotted-wall test section described in Fig. 9.

In order to investigate the capacity for the slotted-wall test section to accommodate various airfoil profiles, the following airfoils were also tested at zero angle of attack: a 12% thick circular arc with $c=5.8$ cm, an NACA 64A010 and an NACA 0012, both with $c=7.6$ cm. Study of the first two airfoils was limited to Schlieren photography. Testing the shorter-chord circular arc airfoil in place of the 7.6 cm circular-arc airfoil resulted in a change in $H/2c$ from 1.0 to 1.31 and in A_f/A_{ts} from 0.060 to 0.046. A shock profile for the 5.8 cm circular arc airfoil at $M=0.86$ is shown in Fig. 10 and is observed to be in good agreement with those obtained for the 7.6 cm chord circular arc airfoil in the slotted-wall test section.

Testing the NACA 64A010 airfoil resulted in $H/2c=1.0$ and $A_f/A_{ts}=0.050$. Shock-wave profiles for this airfoil, for a range of Mach number and $Re_c=2\times10^6$, are compared in Fig. 11 with those observed in the Ames 2×2 ft wind tunnel by Stivers[16] at $Re_c=4\times10^6$ using a 15.2-cm chord length

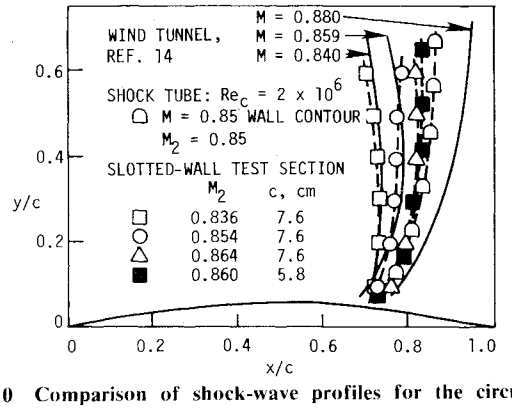

Fig. 10 Comparison of shock-wave profiles for the circular-arc airfoil, $\alpha=0$.

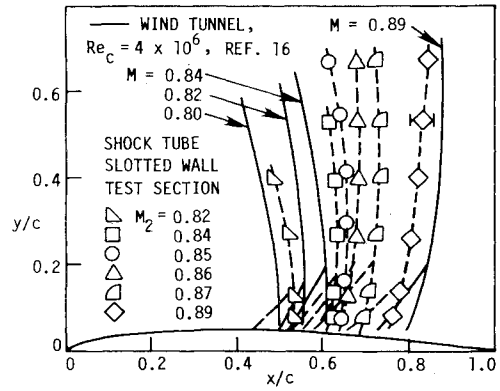

Fig. 11 Shock wave profiles, NACA 64A010 airfoil, $\alpha=0$. Shock-tube $Re_c=2\times10^6$.

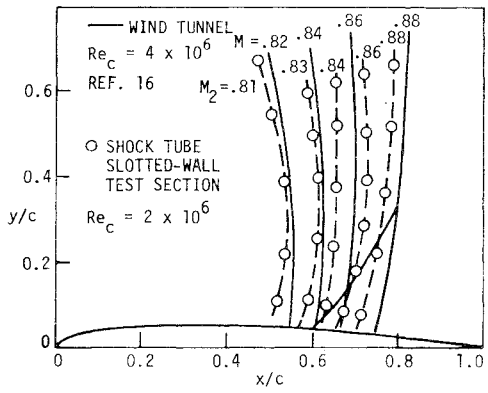

Fig. 12 Shock-wave profiles, NACA 0012 airfoil, $\alpha = 0$.

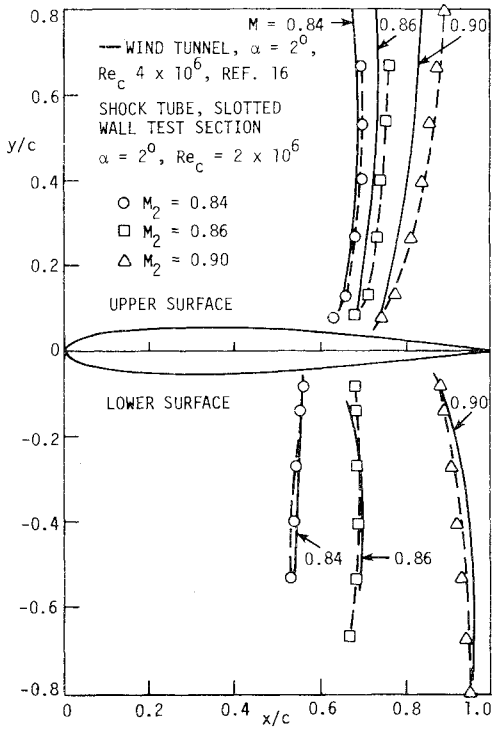

Fig. 13 Comparison of shock wave profiles, NACA 0012 airfoil, $\alpha = 2$ deg.

model. For the most part the agreement between the shock tube and the wind tunnel results is good. The present results reproduce the lamda shock configuration near the airfoil and show the same trends of variation of shock-profile position with Mach number as do the results from the wind-tunnel study.

Testing of the NACA 0012 airfoil in the slotted-wall test section was accomplished by using the same test airfoils that were used in the contoured-wall tests of the 0012 profile. Figure 12 presents a comparison of the shock profiles obtained for the 0012 airfoil and the corresponding wind-tunnel profiles. The agreement between the two sets of profiles is good for the complete range of Mach number. Pressure coefficients vs chord position for the 0012 airfoil tested in the slotted-wall test section at $M_2 = 0.85$ are shown in Fig. 8 as the solid symbols; they are seen to be in good agreement with the wind-tunnel results.

From the results in Figs. 8 and 10-12, it is seen that the shock-tube slotted-wall test section, as described in Fig. 9, has produced good results for the different symmetric airfoil profiles tested at zero angle of attack (i.e., for cases in which the flow about the model is symmetric). In order to investigate

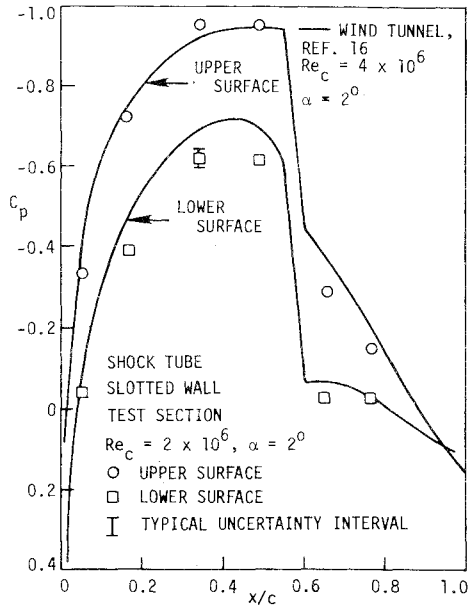

Fig. 14 Pressure coefficients vs chord position, NACA 0012 airfoil, $M = 0.842$, $\alpha = 2$ deg.

the performance of the slotted-wall test section for nonsymmetric flows, the 7.6 cm-chord 0012 airfoil was studied at 2 deg angle of attack. Figure 13 presents a comparison of shock-wave profiles obtained for this case and those observed by Stivers[16] at $\alpha = 2$ deg in the Ames 2 × 2 ft wind tunnel. For the most part the agreement is good. Pressure coefficients vs chord position for the 0012 airfoil are compared in Fig. 14 for the case $\alpha = 2$ deg and $M_2 = 0.842$. Although the shock tube tests indicate slightly higher pressure values for the lower airfoil surface, the agreement between the wind-tunnel and shock-tube results is again good.

The collective results for the three airfoil profiles tested indicate that the slotted-wall shock-tube test section described in Fig. 9 exhibits the desired performance characteristics for test Mach numbers in the vicinity of 0.85.

Conclusions

The results of this study have led to the following conclusions:

1) Steady transonic airfoil flows similar to those observed in conventional wind tunnels can be generated in shock tubes within the available testing time.

2) The test region flow is very uniform and turbulence-free. This is evident from Schlieren photos and from the response of a hot-wire anemometer.

3) Blockage effects due to close proximity of walls to the airfoil model can be alleviated either by test section wall contouring or by use of a properly designed slotted-wall test section. Although the wall contouring method seems to require that contours be matched to each airfoil tested and may not produce flows that are in all respects correct, the method does have the advantage of producing test flows with known boundary conditions and thus provides reference flows useful in analytical and numerical studies. The slotted-wall test section developed in this study produces essentially correct airfoil flows and exhibits testing flexibility, as evidenced by good agreement found for several cases between shock-tube-generated airfoil flow and corresponding airfoil flows observed in conventional wind tunnels.

4) The shock tube has the potential of producing flows with very high chord Reynolds numbers in the transonic range. A shock tube capable fo withstanding high internal pressures is required to produce such Reynolds numbers.

5) Several topics merit further consideration. The matter of model deflection resulting from high dynamic pressures at

high Reynolds numbers should be investigated in detail for shock-tube flows. The inherently short test times for shock-tube flows may also present problems for some flows. Although steady flows were achieved in the present tests, unsteady periodic transonic airfoil flows, of the type observed by McDevitt et al.[17] in other flow regimes, may not be observable in shock tubes due to short test times. Future testing of airfoils at high Reynolds numbers in the shock tube should be undertaken using a test section with both increased airfoil span and test section height. The increased span combined with the decreased sidewall boundary-layer thickness at high Reynolds numbers would minimize possible three-dimensional effects resulting from the presence of the sidewall boundary layer. This approach may be necessary since sidewall boundary-layer removal appears to be difficult due to the short test times. Increased test section height (increased $H/2c$) is desirable to minimize wall interference effects on the transonic flowfield.

Acknowledgments

This study was supported by the Engineering Research Institute at Iowa State University under NASA-Ames Grant NSG-2152. The authors gratefully acknowledge the assistance rendered by M.J. Chaney, an Iowa State University graduate student, in conducting the experimental work associated with this research.

References

[1] Orlik-Ruckemann, K.J. (ed.), "An Overview: Ground Testing and Simulation," *Astronautics & Aeronautics,* Vol. 12, June 1974, pp. 54-60.

[2] Polhamus, E.C., Kilgore, R.A., Adcock, J.B., and Ray, E.J., "The Langley Cyrogenic High-Reynolds Number Wind-Tunnel Program," *Astronautics & Aeronautics,* Vol. 12, Oct. 1974, pp. 30-40.

[3] Geiger, S.W., Mautz, C.N., and Hollyer, R.N., Jr., "The Shock Tube as an Instrument for the Investigation of Transonic and Supersonic Flow Patterns," Engineering Research Institute Rept. Project M720-4, Univ. of Michigan, 1949.

[4] Griffith, W., "Shock-Tube Studies of Transonic Flow Over Wedge Profiles," *Journal of Aeronautical Sciences,* Vol. 19, April 1952, pp. 249-257.

[5] Ruetenik, J.R. and Whitmer, E.A., "Transient Aerodynamics of Two-Dimensional Airfoils," WADC Tech. Rept. 54-368, Part 2, Wright Air Development Center, Wright-Patterson Air Force Base, Ohio, March 1958.

[6] Varwig, R.L. and Rosenman, L., "A 7-Ft-Diameter Shock Tube for Transonic and Supersonic Aerodynamic Testing," *Journal of Spacecraft and Rockets,* Vol. 3, Dec. 1966, pp. 1809-1811.

[7] Glass, I.I. and Patterson, G.N., "A Theoretical and Experimental Study of Shock-Tube Flows," *Journal of the Aeronautical Sciences,* Vol. 22, Feb. 1955, pp. 73-100.

[8] DeRose, C.E., "Trim Attitude, Lift and Drag of Apollo Command Module with Offset Center-of-Gravity Positions at Mach Numbers to 29," NASA TN D-5276, 1969.

[9] Cook, W.J., Persley, L.L., and Chapman, G.T., "Use of Shock Tubes in High-Reynolds Number Transonic Testing," *Proceedings of the Tenth International Shock Tube Symposium,* Kyoto, Japan, 1975, pp. 472-479.

[10] Mirels, H., "Shock-Tube Test Time Limitation Due to Turbulent-Wall Boundary Layer," *AIAA Journal,* Vol. 2, Jan. 1964, pp. 84-93.

[11] Goethert, B.H., *Transonic Wind Tunnel Testing,* Pergamon Press, New York, 1961.

[12] Murman, E.M. and Cole, J.D., "Calculation of Plane Steady Transonic Flows," *AIAA Journal,* Vol. 9, Jan. 1971, pp. 114-121.

[13] Murman, E.M., "Analysis of Embedded Shock Waves Calculated by Relaxation Methods," *AIAA Journal,* Vol. 12, May 1974, pp. 626-633.

[14] Wood, G.P. and Gooderum, P.B.., "Investigation with an Interferometer of the Flow Around a Circular-Arc Airfoil at Mach Numbers Between 0.6 and 0.9," NACA TN 2801, 1952.

[15] Arieli, R., NASA Ames Research Center, private communication.

[16] Stivers, L.S., Jr., NASA Ames Research Center, private communication.

[17] McDevitt, J.B., Levy, L.L., Jr., and Deiwert, G.S., "Transonic Flow About a Thick Circular-Arc Airfoil," *AIAA Journal,* Vol. 14, May 1976, pp. 606-613.